JOURNAL OF CATALYSIS **100**, 59–68 (1986)

Catalytic Activity of Model Aluminium-Doped TiO_2 Catalysts

I. A Study of Promoter Effects on the Decomposition of N_2O

A. BORONICOLOS AND J. C. VICKERMAN

Department of Chemistry, UMIST, P.O. Box 88, Manchester M60 1QD, United Kingdom

Received June 25, 1985; revised November 29, 1985

The influence of Al^{3+} dopents on the catalytic activity of TiO_2 for the decomposition of N_2O has been studied using the solid solution technique. Substitutional solid solutions were prepared up to about 4 at.% Al; between 4 and 10 at.% a two- or three-phase system developed containing the solid solution and a separate corundum phase. The catalysts were well characterised by X-ray diffraction, ESR, conductivity measurements, and Static SIMS. Al^{3+} is shown to generate Ti^{3+} during a complex charge compensation in the TiO_2 lattice. Catalytic activity for N_2O decomposition was little affected by Al doping in $Ti_{(1-x)}Al_xO_2$ up to $x = 0.003$. Between $x = 0.003$ and $x = 0.03$ there was a 10-fold increase in activity. Between $x = 0.03$ and $x = 0.1$ activity fell by a factor 10. The data have been interpreted in terms of the developing electronic interactions between the Ti^{3+} ions generated as a consequence of Al^{3+} doping. It is shown that earlier theories developed to explain the activity of transition metal ions in insulating and semiconducting oxides are applicable to this type of system. © 1986 Academic Press, Inc.

INTRODUCTION

The use of well-characterised model systems to promote our understanding of the behaviour of complex catalysts is recognised to be necessary whether metal or oxide catalysts are being studied. Model oxide solid solution catalysts allow good control of many of the geometric and electronic variables important in controlling catalytic activity. Thus the influence of host lattice and active metal ion have been studied for a wide range of reactions (*1*, *2*). The electronic isolation of active ions, transition metal ions (tmi), in insulator matrices has been shown to promote their activity. Increasing the concentration of tmi to levels where electron exchange becomes significant results in a considerable lowering of catalytic activity. A semiquantitative theory has suggested that the activity fall is a result of decreased availability of electron density at the surface sites due to competition from electron exchange between tmi within the solid (*3*, *4*). The further development of an exchange system as tmi concentration is increased (>1–10%) leads to an increase of surface activity due, it is thought, to the development of collective electron band structure within the tmi sublattice. The probability of acceptor reactant molecules adsorbing and reacting at the surface will be greatly increased if their energy state lies below the Fermi level of the developing sublattice band structure.

These observations and explanations are clear and understandable for model catalysts in which tmi are incorporated in insulating oxides such as α-Al_2O_3, MgO, CaO, or $MgAl_2O_4$. However, many catalyst systems consist of mixtures of semiconducting oxides. It might be expected that ideas of electronic isolation and the development of collective electron properties would not be applicable. However, dopent ions in TiO_2 and SnO_2 do seem to act almost independently of the semiconducting host lattice, and once they are present in sufficient numbers the effect of concentration is very similar to that observed for insulators (*5*, *6*). Thus it is the onset of electron delocalisation *within the tmi sublattice* which causes

0021-9517/86 $3.00

a reduction of activity, and subsequently it is the establishment of a facile conduction band system within that sublattice, apparently independent of the host, that stabilises the adsorbed intermediate and renews surface activity.

So far these studies have centred on understanding the influence of isolation and electron exchange on a tmi which is recognised to be an active centre in many catalyst systems. Many real catalyst systems consist of an active, often semiconducting oxide, in which a promoter is incorporated. The promoter is not usually active of itself; its function is to activate the host lattice. Conceptually in terms of solid solution modelling this is the reverse of the approach so far. However, promoter ions will interact with the electronic state of the catalyst and disrupt or influence it some way. Thus the observed effects should provide a test for the generality of the explanations which have been outlined above.

The purpose of the particular work described here is to explore the effect on N_2O decomposition of incorporating Al^{3+} into the TiO_2 catalyst. Al^{3+} itself is not a recognised component of an active catalyst for N_2O decomposition, so would not of itself be expected to increase the catalytic activity of TiO_2. However, its charge state and electronic configuration will create a disturbance within the TiO_2 lattice. Although effects due to isolated active centres would not be expected, some influence on the collective electron system will be expected and will test the theories so far developed.

Diverging opinions have been expressed as to the structure of aluminum-doped rutile. On the one hand Yahia has proposed a model in which Al^{3+} substitutes Ti^{4+} ions and charge compensation occurs by a hole trapped on a neighbouring oxygen ion (*7*). Førland on the other hand suggested that Al^{3+} dissolves interstitially at reduced pressure (*8*). Between these two views Slepetys and Vaughan thought that charge compensation in Al-doped TiO_2 demanded the presence of both substitutional and interstitial aluminium ions, (*9*). Whilst accepting that this was probably the situation Kerssen and Volger have suggested that interstitial Ti^{3+} ions are also required at higher degrees of reduction (*10*). It is clear that the starting point for this study must be the characterisation of the Al-doped catalysts.

EXPERIMENTAL

The catalysts were prepared by slurrying together TiO_2 (99.95% pure CLD 1231 from Tioxide International Ltd) with calculated quantities of BDH AnalaR aluminum nitrate. The samples were dried at 370 K and then heated at 470 K for 2 h to decompose the nitrate. They were finally calcined at 1230 K for 20 h in an argon atmosphere. As will be shown, solid solution was achieved up to about 4 mol% and above this concentration two phases were evident; however, the catalysts are designated by x assuming substitutional solid solutions, $Ti_{1-x}Al_xO_2$ (the use of this formula does not imply full stoichiometry since the precise concentration of oxygen was not analysed). Thirteen samples were prepared with x ranging from 0 to 0.1.

The catalysts were very fully characterised. Crystal structure was monitored by X-ray diffraction measurements using a Debye–Scherrer camera and Ni-filtered Cu$K\alpha$ radiation. Catalyst surface areas were determined by volumetric adsorption of N_2 at 77 K via the BET technique. Using a Varian E9 spectrometer ESR spectra were obtained with the sample under vacuum and intensities were calibrated using a "strong pitch" sample. Conductivity measurements were carried out on compressed pellets of the catalyst samples using a four probe van der Pauw technique (*11*), which allows dc measurements on powdered samples. Finally measurements of surface composition were obtained using a VG secondary ion mass spectrometer. The sample was bombarded by a very low flux of argon atoms ($<10^{10}$ atoms $cm^{-2}s^{-1}$) at 2 keV energy using a combined ion/atom beam source designed and built at UMIST (*12*). Secondary ions were collected and analysed by a VG 12-12 quadrupole analyser.

The catalytic activity for N_2O decomposition was monitored in a cylindrical quartz reactor of 500 cm^3 volume. The reactor was part of a conventional glass, mercury diffusion pumped, high-vacuum system having a base pressure of 10^{-3} N m^{-2}. The reactor and gas-handling section of the system were protected from mercury contamination by liquid-nitrogen traps. Approximately 0.5 g of catalyst was spread over the bottom of the reactor. The catalysts were first pretreated by outgassing at 1000 K for 18 h at 10^{-2} N m^{-2}. The reactor was then cooled to the chosen reaction temperature and 1.7 kN m^{-2} of medical grade N_2O was admitted to the catalyst. The reaction mixture was continuously monitored via a capillary leak to the head of an AEI MS10 mass spectrometer. Flow through the capillary stabilised within 1 min so reaction temperatures were chosen so that this was not a significant fraction of total reaction time. Between 12 and 20 reactions were studied on each catalyst in the temperature range 770–920 K. Reproducible results were obtained by outgassing at 1000 K for 1 h between runs. The first reaction rate did not usually fit the trend of the subsequent data and was accordingly discarded.

RESULTS

Catalyst Characterisation

The X-ray diffraction data were used to obtain the a_0 and c_0 lattice parameters via the Straumanis technique. Within the Al concentration range studied there was a slight decrease in a_0 from 0.4593 nm and a small but definite increase in c_0 from 0.2956 to 0.2959 nm at $x = 0.04$. For a_0 this is in line with the smaller radius of the Al^{3+} (0.051 nm) ion compared to the Ti^{4+} ion (0.063 nm), and in the case of c_0 suggests that interstitial Ti^{4+} may be the main charge compensating centre. Up to $x = 0.04$ there was no evidence of phases other than rutile, whereas above this level there was also evidence of a corundum phase. This data suggests that solid solution takes place up to $x = 0.04$ and thereafter a two phase system develops as would be expected.

TABLE 1

The Surface Areas and Activation Energies for N_2O Decomposition over the Catalysts $Ti_{1-x}Al_xO_2$

x in $Ti_{1-x}Al_xO_2$	Surface area (m^2 g^{-1})	Activation energies for N_2O decomposition (kJ mol^{-1})
0	3.4	52.5
0.0002	1.3	43.0
0.0003	2.6	50.8
0.001	1.6	24.2
0.002	2.4	52.2
0.003	1.8	48.4
0.004	2.6	52.2
0.008	2.2	85.5
0.031	2.1	85.7
0.044	2.0	59.1
0.067	3.1	70.7
0.083	3.3	67.5
0.100	4.9	53.4

The surface areas of the catalysts are reported in Table 1.

A study of the surface composition of the catalyst should shed light on the uniformity of dispersion of Al in the solid. Figure 1a shows the variation of the secondary ion ratio $Al^+/(Al^+ + Ti^+)$ as a function of composition, x, before and after a 3-min ion etch at 75 μA min^{-1} to yield a measure of the surface and bulk Al concentration. It should be remembered that the sensitivity to Al is approximately 100 times greater than to Ti. An almost linear rise in the ion ratio with x is observed up to $x = 0.03$ for the etched series indicating a uniform incorporation of Al up to this level but thereafter the concentration plateaus. SIMS only measures the top surface concentration. The observation of constant surface concentration whilst the bulk concentration continues to increase suggests that islands of α-Al_2O_3 are being formed at the surface whose depth is increasing more rapidly than their lateral size. There is clearly phase separation of α-Al_2O_3 occurring. Below $x = 0.04$ the steeper rise in the ion ratio as a function of x for the nonetched series indicates some segregation of Al towards

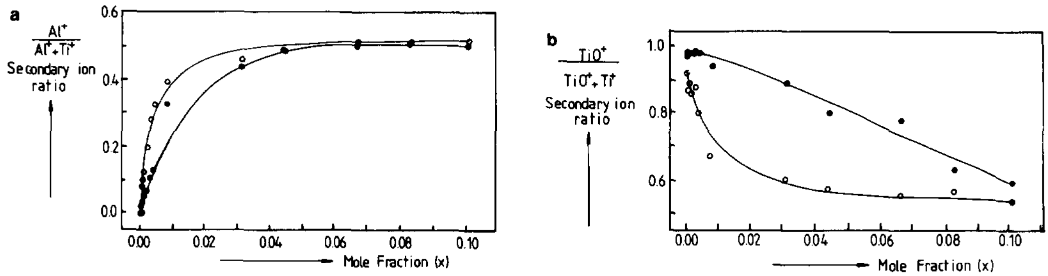

FIG. 1. Variation of secondary ion ratio (a) $Al^+/(Al^+ + Ti^+)$; and (b) $TiO^+/(Ti^+ + TiO^+)$ as a function of Al incorporation in TiO_2, x, before (○) and after (●) a 3-min argon ion etch at 75 μA min^{-1}.

the surface even in the solid solution regime.

The effect of Al incorporation on bonding in the surface of the catalysts can be monitored via the TiO^+ secondary ion where emission is sensitively dependent on the metal–oxygen bond strength (*13*). In Fig. 1b the ion ratio $TiO^+/(TiO^+ + Ti^+)$ is plotted against x again for both ion-etched and non-etched surfaces. It is clear that the bonding of oxygen to Ti is weakened up to $x = 0.01$ in line with the higher concentration of Al in the surface. Beyond $x = 0.03$, as we indicated above, the constant ion ratio is probably a consequence of phase segregation, further Al mainly going to form α-Al_2O_3. However, the variation after etching shows an approximately linear fall with increasing x all the way to $x = 0.1$. This demonstrates that although phase segregation does occur as the concentration of Al increases there is an increase of Al in the solid-solution phase throughout the range up to $x = 0.1$, as indeed would be expected if thermodynamic equilibrium of the Al dispersal was reached during preparation.

Turning to the ESR data, the only signals accessible to study are those due to F-centres (electrons trapped at anion vacancies), $g_0 = 2.0007$, observable at room temperature, and Ti^{3+} ions, $g_{av} = 1.950$, observable only at 77 K. These signals only appear to a significant extent after thermal vacuum outgassing. Exposure of the surface to oxygen results in the loss of the F-centres, presumably due to oxygen adsorption, and loss of a large fraction of the Ti^{3+} signal due to oxidation of surface Ti^{3+} to Ti^{4+}. It is evident therefore that most of these lattice defects reside at the surface. Figure 2 shows the variation of Ti^{3+} with x after outgassing at 770 K for 4 h. It is significant that the form of the curve is rather similar to Fig. 1. Al^{3+} obviously promotes the formation of surface Ti^{3+}. It has been shown in Fig. 1b that Al^{3+} weakens the surface–oxygen bond presumably increasing the probability of oxygen loss from the surface. When oxygen departs from the surface the electrons remaining will be trapped at oxygen vacancies and/or Ti^{4+} interstitials, the concentration of which will have also been increased by Al^{3+} incorporation. Thus an increase in the Ti^{3+} content with Al^{3+} is to be expected.

However, above $x = 0.003$ the Ti^{3+} peak to peak width broadens markedly by a factor of 2 or more from around 230 to 520 G. It is in this region that the linear rise of Ti^{3+}

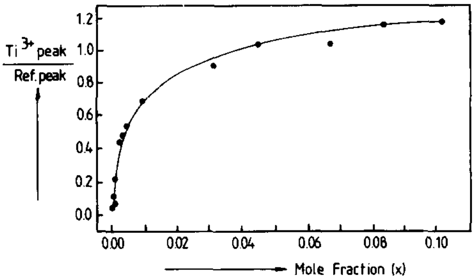

FIG. 2. Variation of the ESR Ti^{3+} signal intensity of catalysts after outgassing for 4 h at 770 K as a function of aluminium incorporation in TiO_2, x.

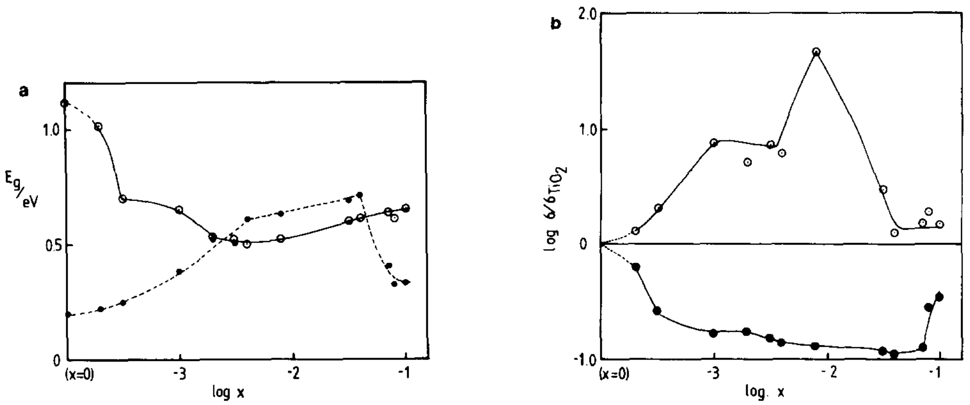

FIG. 3. The variation as a function of Al content, x, of (a) the activation energy for conduction $E_g(=\frac{1}{2}E_{gap})$ for dark (○) and UV conductivity (●) and (b) the relative conductivity at 490 K in the dark (○) and under UV irradiation (●).

intensity with x is lost. Such effects can be partly explained by the development of rapid electron exchange which would cause the peak to partially collapse. Thus Fig. 2 cannot be taken to reflect only changing Ti^{3+} concentration with x. It is probable that the real concentration continues to increase rather more steeply with x although a plateau region is expected beyond $x = 0.04$ due to phase separation effects.

Conductivity measurements, to discover the effect of Al incorporation on the charge transfer properties within TiO_2, were carried out using the van der Pauw four probe technique (*11*). This allows dc measurements to be made on an irregularly shaped though uniformly thick polycrystalline sample, and overcomes the problems of contact resistances at the probe–sample interface. Current is measured via two probes and potential is applied via the other two and then their roles are reversed. The probes are placed at the periphery of the sample and in our case this allowed the effect of UV irradiation to be examined using a mercury arc lamp. The measurements were made in air in the temperature range 300–700 K.

Figure 3a shows the variation of activation of conduction E_g ($= \frac{1}{2}E_{gap}$) for dark and UV conductivity as a function of Al^{3+} content. The activation energy for pure TiO_2 (1.12 eV) is a little lower than expected for a band gap of a little over 3 eV. However, the band gap is known to fall strongly with temperature $E_{gap(T)} = E_{gap} - \beta T$ where $\beta = 6.6\text{–}8.9 \times 10^{-4}$ eV K^{-1} (*14*). Up to $x = 0.01$ there is a very sharp fall in E_g and rise in conductivity (Fig. 3b). Al^{3+}, it has been explained, will give rise to lattice defects to provide charge compensation, namely Ti_I^{4+} and V_0.

These interstitial Ti_I^{4+} and ion vacancies, V_0, will draw electrons from neighbouring O^{2-} sites thus[1]

$$Ti_I^{4+} + O^{2-} \rightarrow Ti_I^{3+} + O^- \qquad (1)$$

$$V_0 + O^{2-} \rightarrow V_0^- + O^- \qquad (2)$$

TiO_2 is thought to be a polaron hopping semiconductor. Thus these new sites will provide new polarons and the polaron hopping distance will be reduced, activation energy will fall and conductivity will rise. Alternatively using the band model we can say that new donor sites, Ti_I^{3+} and V_0^-, are formed in the band gap. Since the concentration of Al^{3+} is small the mobility of charge carriers will not be affected and thus conductivity rises whilst E_g falls strongly.

In the concentration region $0.01 < x < 0.04$ conductivity falls and the activation

---

[1] We have slightly changed the conventional symbolism for the electron content of sites.

energy rises slowly. As Al^{3+} increasingly enters the lattice it will tend to disrupt the polaron hopping between Ti^{3+} sites and hence reduce mobility and increase the activation energy. Furthermore oxygen ions in the vicinity of Al^{3+} ions will be less able to exchange electrons with lattice defects due to the fact that Al^{3+} cannot change its valency easily. Thus increasing numbers of compensating centres, Ti_I^{4+} and V_0, will be stabilised as such, reducing the number of donor sites.

Above $x = 0.04$ conductivity and activation energy are almost unaffected by Al, due presumably to the generation of the two-phase system.

The UV data clarify further features. As expected under irradiation, TiO_2 shows a large increase in conductivity and decrease in E_g. However, the incorporation of Al^{3+} seems to almost destroy the effect of UV irradiation. The conductivity and activation energies revert to the dark levels by $x = 0.001$. This may be because O^{2-} ions associated with Al^{3+} will not be available for excitation to produce electron-hole pairs upon UV irradiation. Beyond $x = 0.06$ photoinitiated conductivity is again evident which seems to confirm that part of the two-phase system contains a component of TiO_2 low in Al^{3+}. In this region perhaps we should think in terms of three phases. A solid-solution phase containing Al^{3+} to $x = 0.04$, an α-Al_2O_3 phase, and a TiO_2 phase containing Al^{3+} to $x = 0.001$, the latter being photoactive.

Catalytic Activity

The initial rates of reaction were found to be first-order in N_2O and on the basis of the transition state theory for a unimolecular surface reaction involving a strongly adsorbed intermediate absolute velocity constants were calculated using the relationship

$$k_{abs} = P(N_2)V/[P(N_2O)At] \qquad (3)$$

where $P(N_2)$ is the pressure of N_2 at time t and $P(N_2O)$ is the initial pressure of N_2O, V is the volume of the vessel (cm^3), A is the surface area (cm^{-2}), and t is the initial reaction time (min) (*15*).

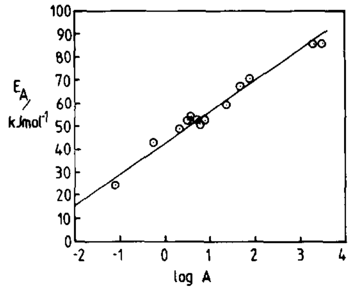

FIG. 4. The compensation effect for N_2O decomposition over aluminium-doped TiO_2 catalysts.

The reaction pressure used here, 1.7 kN m^{-2}, is about a factor 5 less than in previous measurements and consequently the activation energies reflect more closely the energy of the surface reaction excluding the desorption energy for oxygen (*16*). Hence the activation energies reported in Table 1 are some 50 kJ mol^{-1} less than would be expected from earlier data on TiO_2-based solid solutions (*6*). There is, however, a compensation effect exhibited in a plot of activation energy against preexponential factor (Fig. 4) yielding a relationship

$$E_{app}(\text{kJ mol}^{-1}) = 13.5 \log A \ (\text{cm min}^{-1}) + 43. \qquad (4)$$

The variation of N_2O decomposition activity as a function of Al content is shown in Fig. 5 where the rate constants at 900 K are plotted against log x. The comparable data for $Ti_{1-x}V_xO_2$ are shown as a broad dashed line for comparison (*6*). Up to $x = 0.003$ added Al^{3+} causes a small reduction in activity, then between 0.003 and 0.03 there is a large (>10×) increase in activity followed by a sharp fall in activity to $x = 0.1$. It is significant to note that from $x = 0.003$ the behavior of the $Ti_{1-x}V_xO_2$ catalysts was almost exactly the reverse.

In the course of the reaction the N_2/O_2 gas phase ratio was monitored. This should be equal to 2 if all the oxygen is released from the surface, and it will rise if there is significant oxygen retention on the surface. TiO_2 itself retained a large fraction of the

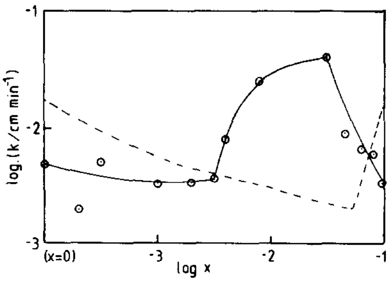

FIG. 5. The variation of activity for N_2O decomposition at 900 K over Al-doped TiO_2 catalysts as a function of catalyst composition, x (○). The comparable data for $Ti_{1-x}V_xO_2$ catalysts are plotted as a broad dashed line.

oxygen produced but as Al^{3+} is added the N_2/O_2 ratio falls rapidly to 2 (see Fig. 6) followed by a small increase again beyond $x = 0.04$. This result provides further clear evidence of the weakening influence of Al on the Ti—O bond strength.

DISCUSSION

The solid-state data give a fairly detailed picture as to the effect of adding small quantities of Al to TiO_2 lattice. As we indicated in the Introduction this system has been studied quite extensively before, and there are diverging views as to the precise defect structure resulting from Al^{3+} doping (*7–10*). Our data shows that

(a) Al_2O_3 does have limited solubility in TiO_2, somewhere about 3%, in good agreement with earlier workers.

(b) Interstitial Ti^{4+} ions may be present from the increase in the c_0 parameter.

(c) On reduction Ti^{3+} ions and anion vacancies are clearly generated whose concentrations are strongly influenced by the Al concentration.

(d) Whilst α-Al_2O_3 solubility is evident up to about $x = 0.04$ there is segregation of Al towards the surface and beyond $x = 0.04$ a two- or perhaps three-phase system results. Whilst it is not possible to be dogmatic we conclude that below $x = 0.03$ much of the Al enters into solid solution in the TiO_2 lattice. Charge compensation is accomplished by interstitial Ti^{4+} and perhaps by some lattice reduction to produce Ti^{3+} ions and anion vacancies. Beyond $x = 0.04$ the surface concentration of Al as measured by SIMS becomes constant which is consistent with the conclusion that islands of α-Al_2O_3 are formed at the surface.

Three general areas of differing behaviour can be discerned as a function of Al content. These correspond closely to the changing catalytic behaviour with Al content. We summarise the salient features of each region.

Aluminium doping $0 < x < 0.003$. In this region Al content rises fairly uniformly throughout the TiO_2 lattice although some segregation to the surface is evident. The Al results in a weakening of the Ti—O bond and an increasing reducibility of the surface to form Ti^{3+} and oxygen vacancies. These changes give rise to increased conductivity and a lowering of the activation energy for charge exchange or polaron hopping from 1.12 to 0.5 eV. The activation energy for conduction of 0.5–0.6 eV for the Al^{3+}-doped ($x > 0.001$) and hence Ti^{3+}-containing samples correlates well with the observation from UPS studies of a new level −0.6 eV below the Fermi level when the (100) face of TiO_2 was thermally reduced (*17*). Associated with the appearance of this level the work function fell from about 5.6 to 4.4 eV. It is possible to combine these observations to construct an energy level diagram for TiO_2 and doped TiO_2 (see Fig.

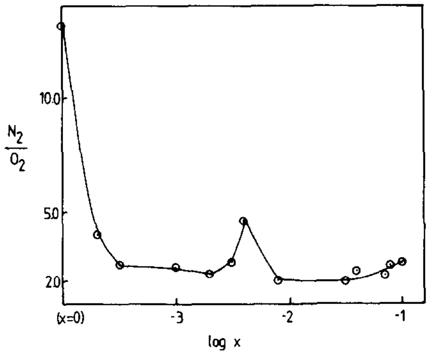

FIG. 6. The variation of the N_2/O_2 ratio as a function of the aluminium content of TiO_2 for the N_2O decomposition reaction (T = 830 K, reaction time 10 min).

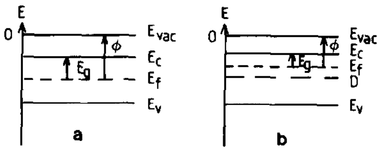

FIG. 7. Energy level diagrams for (a) TiO_2, $\phi = 5.6$ eV, $E_g = 1.2–1.5$ eV; and (b) doped TiO_2, D is the new donor energy level, $E_g = 0.6$ eV and $\phi = 4.4$ eV.

7). The increasing concentration of Ti^{3+} donor sites and the effect of Al^{3+} in locking up O_{2p} electrons will mean that conductivity will be dominated by the donor levels. Although dark conductivity is increased by Al doping, UV conductivity is reduced because the Al^{3+} increasingly deactivates surrounding oxygen ions to excitation by UV radiation.

Aluminium doping $0.003 < x < 0.03$. In this region increasing Al content causes further though less marked increases in surface Al^{3+} and Ti^{3+} content. The activation energy for conduction increases slightly but conductivity itself rises quite markedly. Al^{3+} ions have clearly influenced nearly all the oxygen ions because UV induced conductivity has been lost almost completely. The conductivity and ESR data suggest that the concentration of donor Ti^{3+} is such that a donor *band* will have developed, as indicated in Fig. 7b, and will dominate the charge transfer behaviour. However, we may expect that the presence of Al^{3+} will begin to reduce mobility.

Aluminium doping $x > 0.03$. It is clear that two or three phases have developed in this region. The SIMS data clearly suggest the formation of Al_2O_3 islands with coexisting exposed TiO_2. Thus the phases present are probably an α-Al_2O_3 phase, a doped TiO_2 phase in which the Al content continues to rise slightly and possibly a TiO_2 phase which is only slightly doped. The electronic state of the materials will be dominated by the second phase. The overall conductivity falls quite severely whilst the activation energy rises to 0.65 eV. Concurrent with this is a continuing fall in TiO^+ secondary ion ratio and a small increase in the Ti^{3+} signal from the ESR. These all suggest that the solid solution phase continues to incorporate Al^{3+} and its concentration is such that whilst it promotes the further formation of Ti^{3+}, it disrupts the charge exchange processes causing conductivity to fall.

Catalytic Activity

We now consider how the changing electronic state of the catalysts can explain the changing activity towards N_2O decomposition. In previous publications (*3–6*) we have argued that the activity of these model catalysts can be represented as being the sum of (i) the activity of the host lattice, k_h; (ii) the activity of localised active sites, in the past low concentrations of transition metal ions (tmi), k_l; and (iii) the activity of exchange-coupled sites, in the past tmi at higher concentrations, k_c, i.e.,

$$k_{tot} = k_h + k_l + k_c \qquad (5)$$

It was found that the activity solely attributable to the host fell quite rapidly as tmi concentration rose. k_l, however, rose and passed through a maximum and finally k_c rose at higher dopent concentrations. It has been shown that for insulator and semiconductor hosts

$$k_l = \frac{x}{[\exp(-\Delta E/RT) + 1]} A \exp(-E_a/RT) \qquad (6)$$

where $\Delta E = E_g - E_e$, the difference between the activation energy of conduction, E_g, and the energy required to transfer an electron from the active ion site to the adsorbing molecule, E_e. Clearly as E_g falls below E_e surface activity falls and such a fall in activity has been an almost universal feature of reactions over solid solution catalysts. Since isolated tmi can be thought of as polarons, the concept has been used to derive a plot which qualitatively describes how the activation energy for conduction will decrease with tmi concentration and how, therefore, surface activity may be expected to fall (*6*).

As the concentration of tmi reaches the point where collective electron behaviour is observed, new electron bands due to the tmi will have developed in the host matrix. Volkenstein's ideas are helpful here (*18*). When the energy state of the adsorbing molecule, N_2O^-, falls below the Fermi level of the new band structure, activity can be expected to rise rapidly. Thus we have

$$k_c = \frac{x}{\exp[(E_f - E_{ad})/RT] + 1} A \exp(-E_a/RT) \tag{7}$$

where E_{ad} is the energy level of the adsorbed molecule, for O^- and N_2O^- about 0.8 eV below conduction band, E_f is the Fermi level (which equals E_g when the semiconductor is intrinsic). It has been shown that the variation of the parameters in the denominator qualitatively reproduces the surface activity in this region.

How do these ideas apply when we consider a host lattice doped with a non-tmi species? It is of course the fact that Al^{3+} promotes the formation of lattice defects and in particular Ti^{3+} and anion vacancies which is the crucial factor in modifying surface activity. Thus we are considering a system containing increasing concentrations of Ti^{3+}, a tmi with a d^1 electronic configuration, Al^{3+} and oxygen vacancies. There will be some nonstoichiometry in the host oxide which could account for the rather low E_g, so as Al^{3+} is added the Ti^{3+} concentration will not start from zero, indeed from $x = 0$ to $x = 0.0002$ the $[Ti^{3+}]$ doubles.

Aluminium doping $0 < x < 0.003$. In this region we have an increasing concentration of d^1 ions, a rather similar situation to the V^{4+} in $Ti_{1-x}V_xO_2$ solid solutions (*6*). There is no real evidence of an increase of activity in this concentration range, and this was observed for the vanadium solid solutions. d^1 ions are not expected to be particularly active (*1*). However, unlike the vanadium solid solutions E_g drops very quickly to about 0.5 eV. This is because Ti^{3+} centres form donor levels quite close under the Ti^{4+} conduction band. As we indicated above, the concentration of these Ti^{3+} centres is probably higher than the Al^{3+} concentration so the transition from localised, isolated tmi centres to a delocalised system is rather rapid. The conductivity and activation energy at $x = 0.002$ are of the same order as for $x = 0.02$ in the vanadium system. Thus the fall in activity due to the transition from localised centres to exchange coupled centres is not observed. Perhaps the whole of this region can be regarded as being in such a transitional electronic state.

Although activity only declines slightly, nevertheless the capacity of the various catalyst surfaces to adsorb and retain oxygen changes markedly. The N_2/O_2 ratio drops from about 13 on TiO_2 to just above 2 within this region. This is a startling effect, but it is in line with the variation of the SIMS TiO^+ ratio for the surface. Clearly Al has the effect of weakening the oxygen to surface bond. The influence of this effect on reactivity should be more obvious at higher pressures where the desorption of oxygen will begin to influence continuing activity.

Aluminium doping $0.003 < x < 0.03$. In this region there is a very considerable rise in surface activity by a factor 10 or more, yet we see no sharp change in the activation energy of conduction. Now the precise position of the energy level of adsorbed N_2O^- relative to the Fermi level will be important. In previous studies E_g has continued to vary into the collective region but in this case it is constant and the denominator of Eq. (7), assuming a constant E_{ad} of about 0.8 eV below the conduction band, would yield a constant value of 1. It is clear that the development of collective electron behaviour between the Ti^{3+} ions is correlated with the increase of activity.

However, the actual increase in activity will be mainly influenced by x in Eq. (7). Naturally this should refer to the concentration of Ti^{3+} which is difficult to quantify exactly. It can be seen that between $x = 0.003$ and $x = 0.03$ activity rises by a factor of 10 so there is reasonable correlation between the change in the likely concentration of Ti^{3+} as a consequence of Al^{3+} doping and the activity rise. Thus activity in this concentration region is well described by an increasing number of active tmi sites linked by an efficient electron exchange system.

One further feature of activity in this region is the almost complete elimination of oxygen retention at the surface during reaction. It is difficult to say that this is solely due to weakening of the surface–oxygen bond by the presence of Al^{3+} or to the ease of electron exchange.

Aluminium doping $0.03 < x < 0.1$. In this region there is a very sharp fall in decomposition activity which is correlated with a sharp fall in conductivity and rise in E_g. In a sense the incorporation of more Al^{3+} in the solid solution phase will move the system back to an electronic state intermediate between localised sites and collective sites (Eq. (6)), and as mentioned earlier this leads to a fall in activity because there is competition between charge transfer to the adsorbed molecule and charge transfer in the bulk. Thus Al^{3+} is thought to be disrupting the charge exchange system such that the Ti^{3+} sites are intermediate between collective and isolated sites. Activity would be represented by Eq. (6) for k_l where x may be increasing a little but ΔE will also be increasing, causing k_l to fall.

It could be argued that the fall is solely due to surface alumina. The SIMS data do not suggest a fall in the exposed TiO_2 surface. It would appear that the alumina phase does not encroach too much on the TiO_2 surface.

CONCLUSION

The results discussed in this paper demonstrate that the ideas developed to understand the activity of tmi (not restricted to d^1 ions) in insulating and semiconducting oxides are applicable to understanding the influence on surface activity of doping a tmi semiconducting oxide with *non-tmi* such as Al^{3+}. The dopent Al^{3+} ions initiate the formation of charge compensating tmi of different valency. These ions initially influence the host lattice electronic state and do not themselves introduce additional activity. As Al^{3+} content increases the concentration of tmi charge compensation reaches a level where impurity band formation occurs; the adsorbed intermediate is stabilised relative to this band and activity rises. However, further doping by non-tmi ultimately disrupts the electron exchange system and activity is drastically reduced.

ACKNOWLEDGMENT

A. Boronicolos gratefully acknowledges the provision of a research studentship by Tioxide International.

REFERENCES

1. Cimino, A., *Chim. Ind. (Milan)* **56,** 27 (1974).
2. Vickerman, J. C., *in* "Catalysis" (C. Kemball and D. A. Dowden, Eds.), Vol. 2, p. 107 (Specialist Periodical Report). Chemical Society, London, 1978.
3. Pomonis, P., and Vickerman, J. C., *J. Catal.* **55,** 88 (1978).
4. Pomonis, P., and Vickerman, J. C., "Proceedings, 7th International Congress on Catalysis, Tokyo, 1980," p. 1368. Kodansha/Elsevier, Tokyo/Amsterdam, 1981.
5. Pomonis, P., and Vickerman, J. C., *Faraday Discuss. Chem. Soc.* **72,** 247 (1981).
6. Pomonis, P., and Vickerman, J. C., *J. Catal.* **90,** 305 (1984).
7. Yahia, J., *Phys. Rev.* **130,** 1711 (1963).
8. Førland, K. S., *Acta Chem. Scand.* **20,** 2573 (1966).
9. Slepetys, R., and Vaughan, P. A., *J. Phys. Chem.* **73,** 2157 (1969).
10. Kerssen, J., and Volger, J., *Physica* **69,** 535 (1973).
11. van der Pauw, L. J., *Philips Res. Rep.* **13,** 1 (1958); *Philips Tech. Rev.* **20,** 220 (1958).
12. Brown, A., van den Berg, J. A., and Vickerman, J. C., *Spectrochim. Acta Part B* **40,** 871 (1985).
13. Morgan, A. E., and Werner, H. W., *J. Chem. Phys.* **68,** 3900 (1978).
14. Baumard, J. F., and Tani, E., *Phys. Status Solidi A* **39,** 373 (1977).
15. Laidler, K. J., *in* "Catalysis" (P. H. Emmett, Ed.), Vol. 1, p. 119. Reinhold, New York, 1985.
16. Egerton, T. A., Stone, F. S., and Vickerman, J. C., *J. Catal.* **33,** 299, 307 (1974).
17. Lo, W. J., Chung, Y. W., and Somorjai, G. A., *Surf. Sci.* **71,** 199 (1978).
18. Volkenstein, F. F., "The Electronic Theory of Catalysis on Semiconductors." Pergamon, Oxford, 1963.